Portland Clinker-Fly Ash Cements – Relation between Compressive Strength and Microstructure

Harald Justnes, Klaartje De Weerdt and Tone A. Østnor

Synopsis: Portland cements were made by mixing 4 different clinkers with 2 gypsum levels and 0-5% limestone powder. The compressive strength after 28 days of curing varied from 40 (5802) to 70 MPa (9718 psi) for mortar with equal w/c. Some of the clinkers were replaced with 4 different fly ashes and the response on strength differed. To explain the relatively large differences in strength evolution, the clinker and fly ash composition was investigated by SEM-BSE/EDS, the oxide compositions were determined by XRF and differences in clinker mineralogy determined by XRD Rietveld analysis. The microstructure of hydrated cement pastes of clinker/fly ash was investigated by SEM/EDS.

The highest strength was achieved with the white clinker containing no C_4AF, produced using $CaSO_4/CaF_2$ flux, and therefore contained a higher total calcium sulphate content. The white cement also seemed to contain two calcium aluminate phases with potentially some fluoride in one of them, one probably glassy as Rietveld analysis underestimated C_3A. The C_4AF content of the other clinkers have low reactivity within the 28 days explaining some of the difference. One "fly ash" was actually a fluidized bed ash with higher calcium and sulphate content and different morphology explaining the different behavior from the other fly ashes.

Keywords: clinker, compressive strength, fly ash, microstructure, sulphate

Prof., Dr. Harald Justnes is Chief Scientist at SINTEF Community, Dept. Architecture, Building materials and Structures. He is also Adjunct Professor in "Cement and Concrete Chemistry" at Dept. Materials Technology and Engineering, Faculty of Natural Sciences, Norwegian University of Science and Technology (NTNU). His field of interest covers the chemistry of cement, concrete, admixtures and additives (including polymers) from production, through reactivity, to durability.

Prof., Dr. Klaartje De Weerdt is Professor at Dept. of Structural Engineering, Faculty of Engineering, NTNU. Her research is focused on hydration of cementitious systems as well as their durability. Apart from supervising PhD students, she teaches classes in Building Materials, Concrete Technology and Concrete Construction.

Tone A. Østnor was until recently part of the concrete team at SINTEF Community, but is now regional director for the cement producer NORCEM in Northern Norway.

INTRODUCTION

Cement is a key binder component of concrete production in the building industry. It has started out as a complex hydraulic binder, made up of four main clinker components; alite (Ca_3SiO_5), belite (Ca_2SiO_4), tricalcium aluminate ($Ca_3Al_2O_6$) and ferrite (Ca_2AlFeO_5), which are milled together with gypsum to regulate setting time. In recent years, the production of cement has been identified as the third largest emitter of carbon dioxide (CO_2), accounting for approximately 5 to 8% of the total global anthropogenic emissions, with 60% coming from decomposition of limestone in the raw meal and 40% from fuel to reach clinkerization temperatures of 1450°C (2642°F) for a pure Portland cement. Four main methods are currently in place to mitigate this challenge; 1) switching from fossil fuels to alternative fuels [1], 2) increase efficiencies in factories [1], 3) implementation of supplementary cementing materials (SCMs) replacing cement clinker [1, 2] and 4) carbon capture and storage (CCS) [3]. Among those, clinker partially replaced by SCMs is the most promising on a short term [2], whereby significant reduction in CO_2 emission could be expected depending on how much emission

is associated with the SCM (transport, calcination energy etc.). Replacing cement with SCM will also reduce the amount of raw meal needed per unit cement and increase the cement production volume of a cement plant. Most of the cement produced today has clinker replaced with SCMs with an average global clinker factor of 0.85 in 2003 [4], but higher clinker replacement with a greater variety of SCMs is expected in the near future. The potential SCMs of the future include combustion ashes, slag, calcined clay and limestone. Fly ash is commonly employed in current cements with replacement of 20% in Norway.

However, cement varies in composition, and even more, fly ash, leading to variation in their performance in structures. This paper investigates cements derived from different clinkers and in combination with various fly ashes leading to quite a spread in compressive strength. The objective is to try to explain the difference in strength based on observations in their microstructure. Understanding these variations is important since in the near future, performance in building materials may be measured by for instance CO_2 emission per strength unit or other performance criteria.

EXPERIMENTAL

Materials

The three ground clinkers denoted α, β and γ was received from one commercial cement plant, while the white clinker δ was received from another cement plant. The clinker oxide compositions obtained by XRF are given in Table 1, while the mineral compositions derived by Rietveld analysis of X-ray diffraction [5] and simple Bogue calculations are shown in Tables 2 and 3, respectively. Laboratory grade gypsum was used to regulate setting of the clinkers. Limestone powder containing 81% $CaCO_3$ was used to possible induce a synergic effect with calcium aluminate hydrates from the clinker hydration [6]. The three fly ashes in the study was received from different coal fired energy plants and denoted A, B and C, while the fourth ash was from a fluidized bed combustion plant and denoted as D. The chemical compositions of the ashes from XRF are listed in Table 4, while the composition

of the glass phases of the ashes are calculated after crystalline phases are subtracted by Rietveld analyses of XRD profiles [5]. Fly ashes denoted A, B and C comply with class V (siliceous fly ash) in the cement standard EN 197-1:2011, but not fly ash denoted D due to high calcium sulphate content.

Extraction of interstitial phases of clinkers

The extraction procedure involves adding 5 g dry cement to a solution of 25 g maleic acid dissolved in 125 g methanol. After stirring for 10 minutes, the solution is filtered off and the residue washed with 50 ml methanol. Both maleic acid and methanol were of pure laboratory grade. The procedure removes C_3S and C_2S from the clinker.

Mortars

The mortars consisted of 1 part cement, 3 parts European standard graded sand according to EN 196-1 and de-ionized water until w/c = 0.50. The mixing was performed according to the European Norm EN 196-1 and the mortar was cast in sets of three 40x40x160 mm (1.57x1.57x6.30 in) prisms (0.768 litre or 26 fl oz). The standard procedure is to test the flexural strength in 3-point bending for 3 prisms in parallel and the compressive strength on the 6 resulting end-pieces using a 40x40 mm (1.57x1.57 in) metal plate so the compressive strength will be like being measured on a 40 mm (1.57 in) cube. For testing at 1 day the mortars are stored in the mould at 20°C (68°F) , while for later ages they are demoulded after 1 day and cured at 20°C (68°F) and 90% RH.

Scanning electron microscopy

One sample from all the mortar mixes cured for 28 days were cast in epoxy resin, plane polished to achieve a cross-section of the material and sputtered with carbon.

A JEOL JSM-7001F field emission scanning electron microscope combined with a Genesis energy dispersive spectrometer (EDS) operated at an accelerating voltage of 15 kV was used for the SEM-EDS analysis of mortars. In each sample 120-150 EDS point analyses were performed.

X-ray diffraction (XRD)

X-ray diffraction (XRD) scan using a Bruker AXS D8 Focus with a Lynx eye super speed detector operating at 40 kV and 40 mA. A CuK_{α} source (λ = 1.5418 Å) with a 0.2 mm slit was used. The scan was performed between 5 and 75° 2θ with an increment of 0.02 and a scanning speed of 0.5 s/step. The samples were front loaded.

X-ray fluorescence (XRF)

After heating for mass loss on ignition (LOI), the powder is made into a tablet by melting with borax and the content of elements detected by BRUKER S8 Tiger 4 kW X-ray spectrometer.

RESULTS AND DISCUSSION

In Fig. 1 showing the 28 day compressive strength of mortars based on ternary cements made of clinker, gypsum and limestone at equal w/c, it is evident that particularly clinker δ achieves a much higher strength than the other clinkers. Not only was the compressive strength of mortar with clinker δ higher (67 MPa or 9718 psi for 3% gypsum and no limestone) than for clinker α (40 MPa or 5802 psi for 3% gypsum and no limestone) after 28 days curing at 20°C (68°F) submersed in lime saturated water, but the difference was also large when demoulding at 1 day (27.5 MPa, or 3989 psi, for δ versus 15.0 MPa, or 2176 psi, for α clinker). At the same time there is a quite large discrepancy between the C_3A content of clinker δ estimated by Bogue calculations (10.3% in Table 3) from the chemical compositions in Table 1 and that observed by Rietveld analyses of XRD (3.2% in Table 2) compared with the other clinkers (α, β and γ). Therefor the microstructure of clinker δ was investigated closer [7] in order to find reasons for the higher strength development as well as to identify any other aluminate containing compounds than those assumed by Bogue calculations. For instance, the formation of a glassy (no-crystalline) calcium aluminate not observable by XRD put forward as a hypothesis to explain the discrepancy between Rietveld and Bogue calculations. The X-ray diffractogram of the interstitial phases of clinker δ in Fig. 3 shows indeed a bump indicating amorphous phase, but also anhydrite (marked A). There are also possible very small amounts of mayenite, $C_{12}A_7F_2$, and most certainly fluorellestadite, $Ca_{10}(SiO_4)_3(SO_4)_3F_2$, even its major peaks have partial overlap with anhydrite. There is absolutely no trace of C_4AF (as expected for a white clinker) as this phase would have given rise to a peak at about 12° 2θ. The SEM analyses of clinker grains [7] also showed that the interstitial phases of clinker δ consisted of two shades of grey; one lighter with atomic ratio Ca/Al = 1.71 and a darker one with Ca/Al = 1.26. The darker phase contained 0.9 atom% fluorine (F) as revealed by WDS (0% in the light grey phase) and more magnesium (3.0 atom% Mg) than the light grey phase (1.3 atom% Mg). This is a proof that anhydrite and possibly some fluoride were used as fluxes in the production of clinker δ. Analyses of elements by wavelength dispersive spectra (WDS) is more accurate that energy dispersive spectra (EDS) in SEM. The higher

28-day strength of clinker δ is thus caused by a combination of high C_3S content (but β clinker is close to same content) with a high reactive alumina and additional sulphate from flux giving more ettringite with additional bound water.

Clinker δ is also the only clinker with a positive strength response to added limestone, as seen from Fig. 1, due to the so called synergy effect [6]: Depending on the ratio of reacted C_3A to gypsum ratio, the end result is a mixture of ettringite and sulphate-AF_m as the major alumina-bearing phases. But when calcium carbonate is added to the system, carbonate-AF_m is formed rather than sulphate-AF_m and ettringite is stabilized. Since then more ettringite (most sulphate end up there) is formed with more crystal water than in AF_m (32 vs. 12) in addition to the 11 crystal water in carbonate-AF_m, there will be an overall higher amount of liquid water transformed to crystalline with lower porosity and higher strength as a result as calculated from Eq. 1 using cement chemist's short hand notation where C = CaO, A = Al_2O_3, H = H_2O, $\underline{C}$ = CO_2 and $\underline{S}$ = SO_3.

$$2\,C\underline{C} + 3\,C_4A\underline{S}H_{12} + 18\,H = 2\,C_4A\underline{C}H_{11} + C_6A\underline{S}_3H_{32} \quad (1)$$

m = 1.00 g	9.33	1.62	5.68	6.27	[1 g = 0.0353 oz]
M =100.09 g/mol	622.52	8.02	568.50	1255.11	[1 g/mol = 0.0353 oz/mol]
n = 9.99 mmol	14.99	9.91	9.99	5.00	
ρ = 2.67 g/ml	2.015	0.998	2.17	1.778	[1 g/ml = 0.578 oz/in^3]
V = 0.375 ml	4.630	1.623	2.618	3.526	[1 ml = 0.0610 in^3]

According to the reaction in Eq. 1, 100 g (3.53 oz) calcium carbonate (≈1 mol) would bind 162 g (5.71 oz) or ≈9 mol extra water. The total increase in volume of solids will then be ((3.526+2.618)-(0.375+4.630))·100 vol%/(0.375+4.630) = 22.8 vol%.

Further regarding the higher 28-day strength of the δ-clinker, the other clinkers contain a substantial amount of C_4AF (> 10%) that is very slowly reactive and substantial amounts has still not reacted at

28 days and thereby not contributed to strength. Unreacted C_4AF appear as nearly white phases in association with reacted cement grains in the back scattered electron (BSE) images by SEM in Figs. 4-7.

Clinker δ gives higher 1-day strength than the other clinkers because it contains anhydrite as flux and therefore has a total higher calcium sulphate content than the other cement when the same amount of gypsum is added to the clinkers to make cements. Clinker δ also has a higher C_3A content (≈ 6%) than predicted from the Rietveld analysis and part of it probably as a glassy XRD amorphous phase with some fluorine, and there is a potential of forming more ettringite with high water binding capacity early. Clinker δ only has a marginally higher surface than the other clinkers, but substantially higher C_3S content (63.6% according to Rietveld analysis) compared to for instance α (49.1%) that will add to the higher early strength together with excess calcium sulphate not bound early by C_3A being able to help accelerate C_3S hydration [8, 9].

As seen from Fig. 2 for clinker δ, it was also found that in particularly one of the four ashes (ash D) combined with the different clinkers [5] gave higher strength than the others, so the second objective was to find the reason for this through investigation of the microstructure of the mortars tested for strength. Ash D also deviated strongly from ashes A, B, and C in its total chemical composition as shown in Table 4 (more calcium and sulphate) as well as in its glass compositions in Table 5 (more calcium and aluminate, less silicate). The origin of ash D was different as it came from fluidized bed combustion rather from the usual coal fired energy plants as the fly ashes A, B and C. The fly ash response was compared with calcine marl (clay with 20% calcium carbonate) in Fig. 2 and the strength gain is higher due to faster reaction induced by higher specific surface and smaller particles with less glassy nature [10].

Of all the mortars cast, three were selected for closer investigation of their microstructure. Their compositions are given in Table 6. The reasons for this selection was that clinker δ resulted in a

considerable higher strength than clinker β (see Fig. 1) and that the strength increase observed when replacing 5% C fly ash with 5% limestone powder is relatively larger for the β clinker (+13% [5]) than the δ clinker (+5% [5]).

Fig. 4 displays an overview and a close-up of the microstructure of the binder of mortars based on mixes 45, 47 and 63. It is clear that the clinker δ displays a higher degree of hydration than clinker β as seen from less nearly white (light grey) particles being unreacted cement grains, in particular belite, and white particles being unreacted ferrite phase (C_4AF). A higher degree of hydration will of course lead to higher strength gain at equal w/c since more liquid water is transferred to solid hydrates with reduced porosity as a result. Calcium hydroxide is seen as irregular, light grey areas in the close-ups of mix 45 and 63. In the close-up of mix 63, an AF_m phase is clearly seen as a darker grey "triangle" in the upper left quadrant of the image. As seen the close-up of mix 47, a part of the binder looks like a mixture of light and dark, irregular phases. The dark phase had composition in atom% of 26.7 Ca, 6.7 Si, 5.4 Al and 4.5 S; a CASH high in sulphate, while the lighter grey phase had 24.7 Ca, 7.40 Si, 3.40 Al and 1.4 S; a CASH low in sulphate. The extra sulphate comes from the fly ash D containing 6.6% SO_3 (Table 4). A number of carbonate-AF_m phases was detected in the BSE (backscattered electron) images of Fig. 4 as confirmed by elemental analysis by wavelength dispersive spectroscopy (WDS).

Two hundred energy-dispersive spectra (EDS) was taken randomly from 4 selected areas of mix 45, 4 areas from mix 63 and 5 areas from mix 47. One selected area from each mix is shown in Figs. 5 (mix 45), 6 (mix 63) and 7 (mix 47). During a SEM-EDS point analysis the elemental composition of the volume of approximately 1 um^3 is analyzed. This volume can comprise a mixture of different phases. In order to interpret EDS point analysis results, the elemental ratios in that point are calculated and they are plotted in a graph together with the ideal composition of typical cement hydration phases. If a point contains a mixture of phases it will be positioned in between the points indicating the ideal composition of these phases. The advantage of SEM-EDS compared to e.g. XRD is that the phases

do not need to be crystalline. Therefore, the chemical composition of the main hydration phase of Portland cement, amorphous CSH, can be analyzed with this technique.

The general observations from the 13 selected images from mixes 45, 63 and 47 are that

1. All mortars contain ample calcium hydroxide for further pozzolanic reaction
2. There are more unreacted cement grains in mortar based on clinker β than clinker δ, but this is mostly unreacted C_4AF (the least reactive phase) that is not present in clinker δ.
3. Fly ash denoted C consists of the classical alumina-silicate glass spheres still present as unreacted particles embedded in the matrix, while what is left of fly ash D is irregular particles with quite an open structure seen from new crystals growing inside it.
4. There is a tendency of more pores filled with AF_t/AF_m phases when fly ash D is employed that can be due to its much higher sulphate content and potential higher reactivity due to its less glassy nature and more open structure. Its glassy phase also contained more calcium and alumina than the fly ashes (see Table 5).

Different compositional plots from all the EDS spectra are depicted in Figs. 8 (Al/Ca vs. Si/Ca), 9 (S/Ca vs. Al/Ca) and 10 (S/Ca vs. Si/Ca), and compared to the points given for specific compounds like calcium hydroxide (CH), AF_t (ettringite), sulphate-AF_m and carbonate-AF_m, as well as area for CSH-gel.

From Figs. 8-10 the composition of the CSH in the different tested mixes can be determined. In Table 7 the elemental ratios of the CSH phase are given. It should be noted that CSH is a heterogeneous phase and the ratios reported in Table 7 should therefore be interpreted with care. Some clear trends regarding the CSH in the different tested mixes can however still be detected:

- *clinker type – mortar 45 vs. 63 (β vs. δ clinker with fly ash C):*
    - no significant difference in Al/Ca and Si/Ca ratio depending on the clinker type

  - slightly higher sulphate uptake in the CSH for clinker δ, probably because it contains more calcium sulphate since anhydrite was used as flux

- *fly ash type – mortar 45 vs. 47 (fly ash C vs. fly ash D in clinker β)*
  - Fly ash D results in a significantly higher Al/Ca ratio, hence higher aluminate uptake in the CSH compared to fly ash C since the glass composition of fly ash D contains most Al_2O_3 (see Table 5). The Ca/Si ratio stays however similar (1.47-1.59).
  - Fly ash D results in a significantly higher sulphate uptake in the CSH compared to fly ash C, probably because it contains much more sulphate (6.6.% SO_3) than the other (0.2 % SO_3) as seen from Table 4.

From Fig. 2 it can be seen that the synergic strength effect [5] of replacing 5% of fly ash with limestone filler is less for fly ash D (+2.3%) than for fly ashes A (+4.5%), B (+5.5%) and C (+4.4 %). This is probably due to the higher sulphate content of fly ash D leading to a higher fraction of reacted alumina being occupied as ettringite to begin with. Ettringite is stable towards calcium carbonate, only sulphate-AF_m will convert to carbonate-AF_m in contact with calcium carbonate.

CONCLUSIONS

Clinker δ gives higher early strength than the other clinkers because it contains anhydrite as flux and therefore has a total higher calcium sulphate content than the other cement when the same amount of gypsum is added to the clinkers to make cements.

Clinker δ also has a higher C_3A content (≈ 6%) than predicted from the Rietveld analysis and part of it probably is a glassy XRD amorphous phase with some fluorine (also added as flux).

Clinker δ only has a marginally higher surface than the other clinkers, but substantially higher C_3S content that will add to the higher early strength together with excess calcium sulphate not bound early by C_3A being able to help accelerate C_3S hydration.

The higher 28-day strength of clinker δ is a combination of high C_3S content with a high content of reactive alumina and additional sulphate from flux giving more ettringite with additional bound water.

The other clinkers contain a substantial amount of C_4AF that is very slowly reactive and substantial amounts had still not reacted at 28 days and thereby not contributed to strength.

The reason why fly ash D gives higher contribution to strength than the other fly ashes is that fly ash D contains considerable more sulphate (6.6% as SO_3) than the other fly ashes (fly ash B is the second highest with 0.5% SO_3) which would lead to more ettringite formed on the expense of AF_m resulting in more water bound and hence higher strength.

Fly ash D is however not a regular fly ash, but a fluidized bed ash that consist of a much more open structure than the closed glassy, spherical particles of the other fly ashes. It also contains a lot more calcium oxide (17.9% CaO) than the other fly ashes (Fly ash B is the second highest with 7.1% CaO). Hence it is assumed to be more reactive than the other ashes.

The higher sulphate content for fly ash D compared to the other fly ashes also leads to a less response of this fly ash to the synergy effect with limestone since more aluminate will be occupied as ettringite and less available to form carbonate-AF_m.

REFERENCES

[1] Chinyama, M.P.M., 2011, "Alternative fuels in cement manufacturing", DOI 10.5772/22319. https://www.intechopen.com/books/alternative-fuel/alternative-fuels-in-cement-manufacturing

[2] Justnes, H., 2015, "How to Make Concrete More Sustainable", Journal of Advanced Concrete Technology, 13, 147-154

[3] Bosoga, A., Mazek, O. and Oakey, J.E., 2009, "CO_2 Capture Technologies for Cement Industry", Energy Procedia, 1(1) 133-140

[4] Schneider, M., Romer, M., Tschudin, M. and Bolio, H., 2011, "Sustainable Cement Production – Present and Future", Cement and Concrete Research, 41 (7) 642-650

[5] De Weerdt, K., Østnor, T.A., Justnes, H., Ben Haha, M. and Kjellsen, K.O., 2013, "Fly-ash limestone synergy in triple cement". Proceedings of the 1st International Conference on Concrete Sustainability, Paper S2-2-4, pp. 510-515, May 27-29, 2013, Tokyo, Japan (ISBN 978-4-86384-041-6-C3050).

[6] De Weerdt, K., Kjellsen, K.O., Sellevold, E.J. and Justnes, H., 2011, "Synergy between Fly Ash and Limestone Powder in Ternary Cements", Cement and Concrete Composites Vol. 33, No. 1, pp. 30-38.

[7] Justnes, H., De Weerdt, K., Østnor, T.A., 2019, "Relation between strength of cements based on different clinkers and their microstructure", 15th International Congress on the Chemistry of Cement (ICCC), 16-20 September 2019, Praha, Czech Republic, Paper No. 66, 9 pp.

[8] Justnes, H., 2018, "Alternative Setting Retarders for Portland Cement Clinker", Proceedings of the 20th International Conference on Superplasticizers and Other Chemical Admixtures in Concrete, ACI SP-329, Beijing, China, 28-31 October 2018, paper SP-329-17, pp. 201-211 (ISBN-13: 978-1-64195-029-9).

[9] Ménétrier, D., Jawed, I., Skalny, J., 1980, "Effect of gypsum on C_3S hydration", Cement and Concrete Research, Vol. 10, pp. 697-701

[10] Justnes, H., Østnor, T., Danner, T., 2011, "Calcined Marl as Effective Pozzolana", Proceedings of the International RILEM Conference on Advances in Construction Materials Through Science and Engineering, RILEM PRO 79, 5-7 September, 2011, Hong Kong, China, 8 pp.

List of Tables:

List of Figures:

Fig. 5 - Microstructure of mortar sample 45; 65% β clinker + 30% fly ash C + 5% limestone

Fig. 6 - Microstructure of mortar sample 63; 65% δ clinker + 30% fly ash C + 5% limestone

Fig. 7 - Microstructure of mortar sample 47; 65% β clinker + 30% fly ash D + 5% limestone

Fig. 8 - Al/Ca ration as function of Si/Ca ratio of the EDS point analyses of the different blended cements tested. This graph serves to identify the Ca/Si ration of the CSH and the aluminate uptake of the CSH as Al/Ca. In addition, AFm and AFt phases can be distinguished. Points from matrix of mortars 45, 63 and 47 are plotted here as diamond, square and triangles, respectively.

Fig. 9 - S/Ca ration as function of Al/Ca ratio of the EDS point analyses of the different blended cements tested. This graph serves to identify the sulphate containing AFm and AFt phases (AFt = ettringite, AFm_S = monosulphoaluminate and AFm_C = monocarboaluminate). Points from matrix of mortars 45, 63 and 47 are plotted here as diamond, square and triangles, respectively.

Fig. 10 - S/Ca ration as function of Si/Ca ratio of the EDS point analyses of the different blended cements tested. This graph serves to identify the Si/Ca ratio of the CSH and the sulphate uptake in the CSH. AFm represents monosulphate in this graph. Points from matrix of mortars 45, 63 and 47 are plotted here as diamond, square and triangles, respectively.

Table 1 - Chemical composition (%) and physical properties of the clinkers

Cements	**α**	**β**	**γ**	**δ**
SiO_2	20.3	21.3	21.8	23.4
Al_2O_3	5.7	5.4	4.3	4.0
Fe_2O_3	3.3	3.9	5.6	0.2
CaO	61.3	63.5	61.4	67.0
MgO	2.9	1.9	2.1	1.1
K_2O	1.2	0.4	0.4	0.5
Na_2O	0.5	0.3	0.3	0.0
SO_3	1.5	0.4	1.2	1.6
LOI 950°C	1.9	0.5	0.5	0.7
Sum above	98.6	97.6	97.6	98.5
Blaine (m^2/kg)	449	432	426	457
Blaine (in^2/oz)	19760	19000	18750	20100
Density (g/cm^3)	3.1	3.1	3.2	3.1
Density (oz/in^3)	1.8	1.8	1.8	1.8

Table 2 - XRD-Rietveld analysis of the clinker phases (%) [5]

cements	**α**	**β**	**γ**	**δ**
C_3S	49.1	59.9	45.6	63.6
C_2S	25.6	18.8	33.3	30.3
C_3A	10.0	4.6	0.3	3.2
C_4AF	10.2	14.1	18.5	0.0
Sum	94.9	97.4	97.7	97.1

Table 3 - Mineral composition of the clinkers from Bogue-calculations based on the oxide compositions in Table 1.

cements	**α**	**β**	**γ**	**δ**
C_3S	52.3	54.8	47.4	67.8
C_2S	18.8	19.8	26.8	16.0
C_3A	9.5	7.7	1.9	10.3
C_4AF	10.0	11.8	17.0	0.6
Sum	94.9	97.4	97.7	97.1

Table 4 - Chemical composition (%) and physical properties of the fly ashes

Fly ash	**A**	**B**	**C**	**D**
SiO_2	52.9	47.6	53.7	38.7
Al_2O_3	26.4	27.8	22.7	19.6
Fe_2O_3	6.3	5.5	5.7	6.0
CaO	3.3	7.2	5.1	17.9
MgO	2.8	2.3	2.3	2.0
K_2O	3.0	1.4	2.1	2.5
Na_2O	1.0	0.6	1.0	0.7
SO_3	0.2	0.5	0.2	6.6
LOI	1.8	3.3	4.5	3.4
Sum above	97.7	96.2	97.3	97.4
Blaine (m^2/kg)	250	400	395	734
Blaine (in^2/oz)	11000	17600	17380	32300
Density (g/cm^3)	2.2	2.4	2.3	2.6
Density (oz/in^3)	1.3	1.4	1.3	1.5

Table 5 - Glass composition (%) of the fly ashes [5]

Fly ash	**A**	**B**	**C**	**D**
SiO_2	38.0	30.1	39.4	26.3
Al_2O_3	15.6	10.3	13.9	19.6
Fe_2O_3	4.3	5.5	6.6	6.6
CaO	2.4	5.6	4.7	11.5
MgO	2.8	2.3	2.3	2.3
K_2O	3.0	1.4	3.0	3.0
Na_2O	1.0	0.6	0.5	0.5
Sum above	67.1	55.9	70.4	69.8
total amorphous	*69.6*	*59.1*	*73.2*	*64.5*

Table 6 – Composition of mortars selected for microstructure studies

Mix 45	65% β-clinker	30% fly ash denoted C	5% limestone filler
Mix 47	65% β-clinker	30% fly ash denoted D	5% limestone filler
Mix 63	65% δ-clinker	30% fly ash denoted C	5% limestone filler

Table 7 - The composition of the CSH phase in the different mortars

Approx. composition CSH	**45:** β+FA C	**63:** δ+FA C	**47:** β+FA D
Si/Ca	0.63	0.63	0.68
Al/Ca	0.09	0.08	0.15
S/Ca	0.25	0.30	0.50

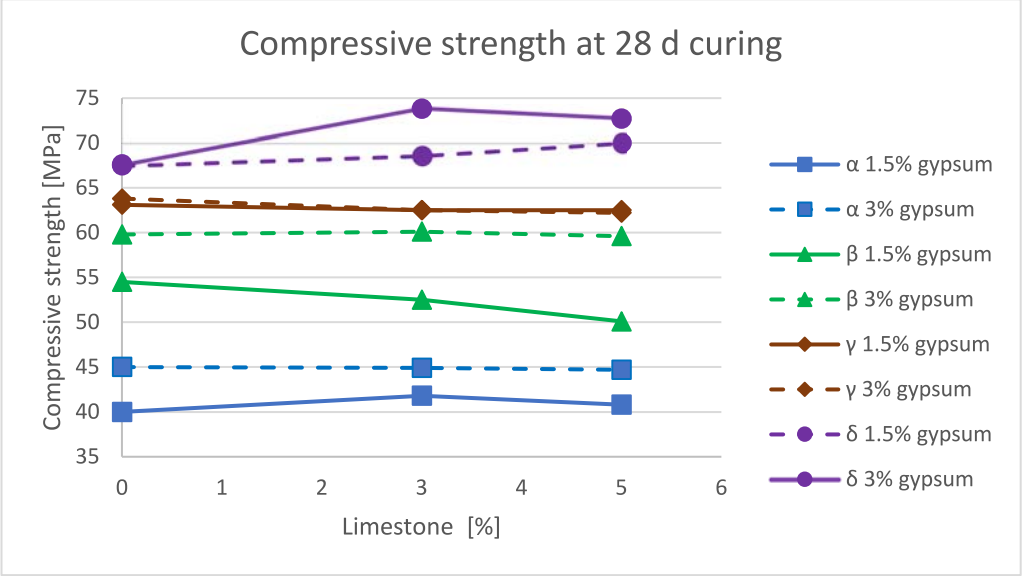

Fig. 1 - Comparative plots of compressive strength at 28 days for all clinkers with 2 levels of gypsum as a function of limestone powder content (1MPa = 145 psi).

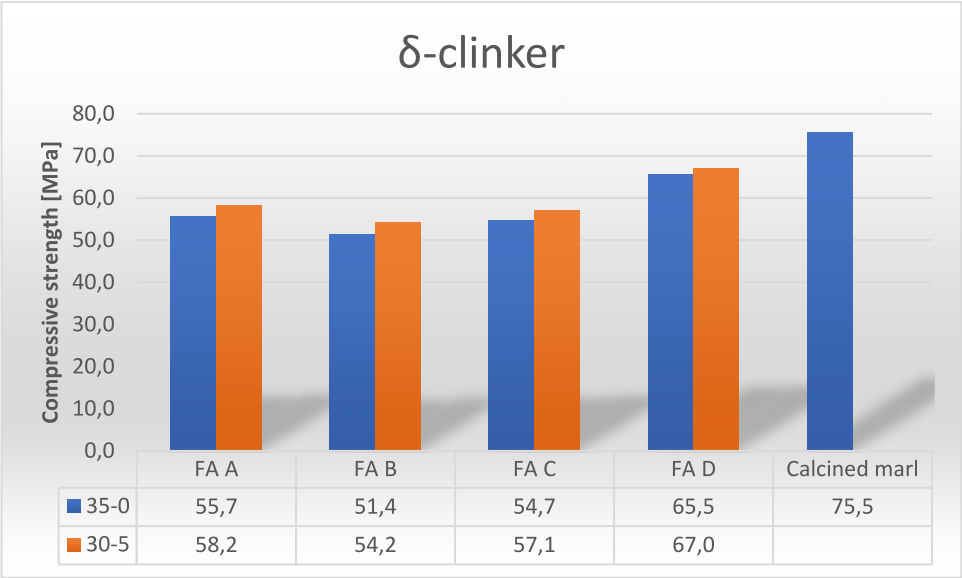

Fig. 2 - The effect of different fly ashes on the compressive strength of clinker δ and their response to combination with lime stone powder. 35-0 = 35% fly ash only, while 30-5 = 30% fly ash combined with 5% lime stone.The result is also compared to 35% calcined "marl" [10] replacing the clinker with 3% gypsum (1MPa = 145 psi).

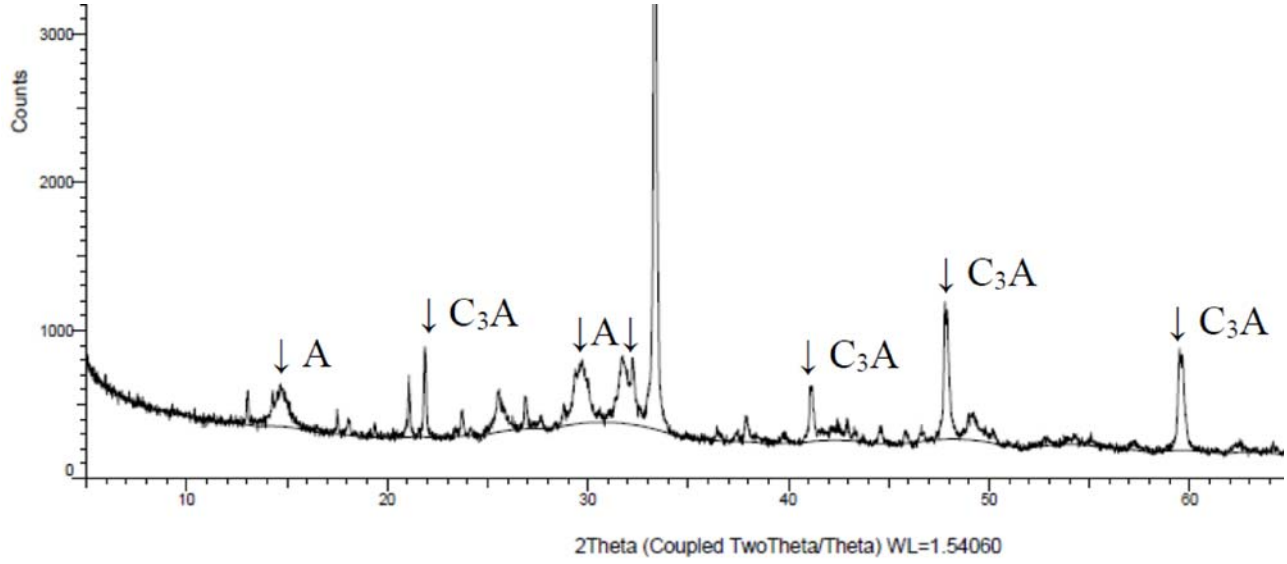

Fig. 3 - XRD profile of interstitial phases from clinker δ after the extraction process. Peaks marked "A" are anhydrite.

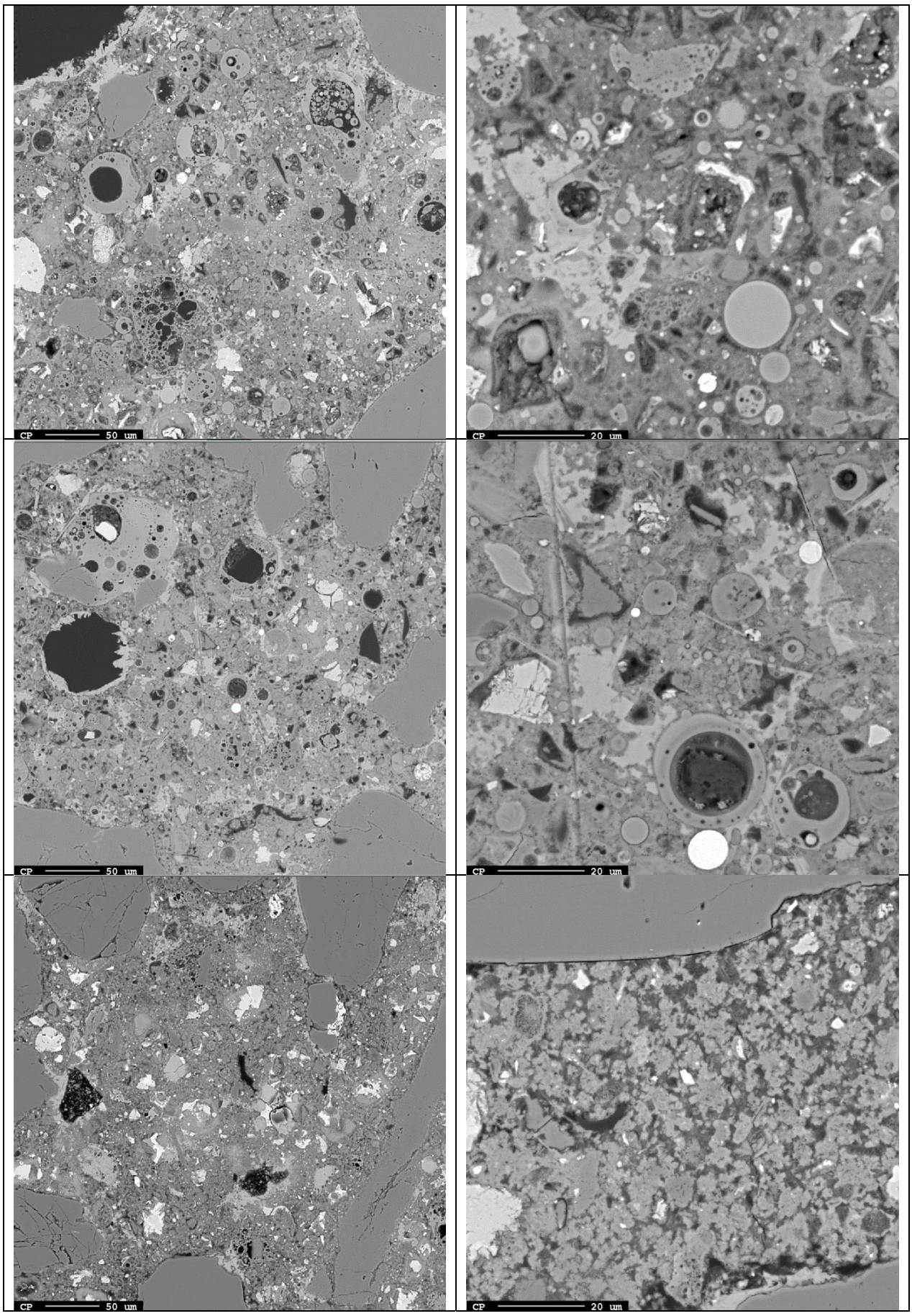

Fig. 4 – An overview (left column) and a close-up (right column) for from top down; mix 45 (65% β clinker + 30% C fly ash + 5% limestone), mix 63 (65% δ clinker + 30% C fly ash + 5% limestone) and mix 47 (65% β clinker + 30% D fly ash + 5% limestone). Rounded particles are fly ash, but they can also be cellular, irregular grains.

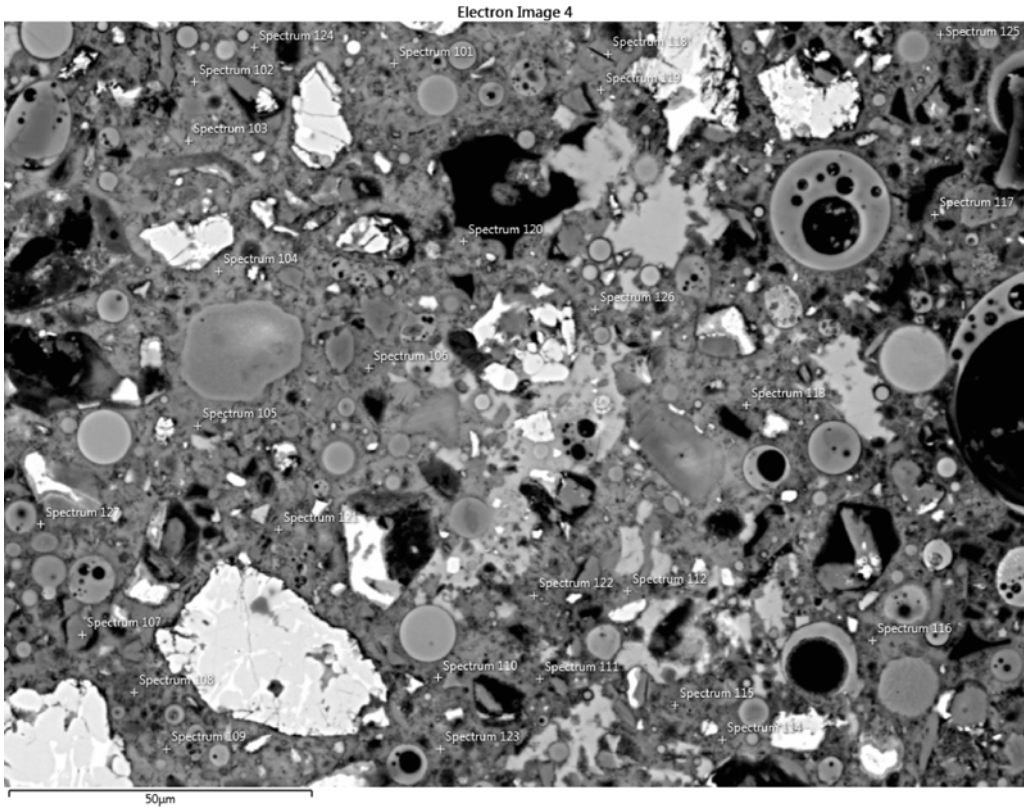

Fig. 5 - Microstructure of mortar sample 45; 65% β clinker + 30% fly ash C + 5% limestone

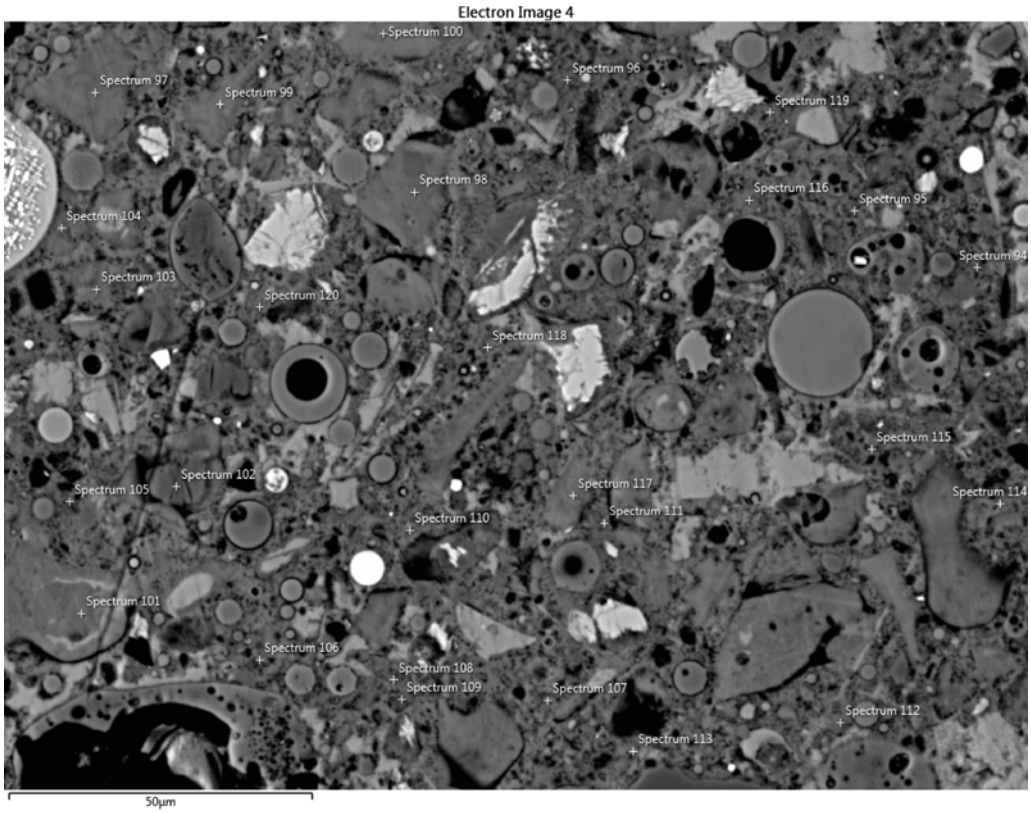

Fig. 6 - Microstructure of mortar sample 63; 65% δ clinker + 30% fly ash C + 5% limestone

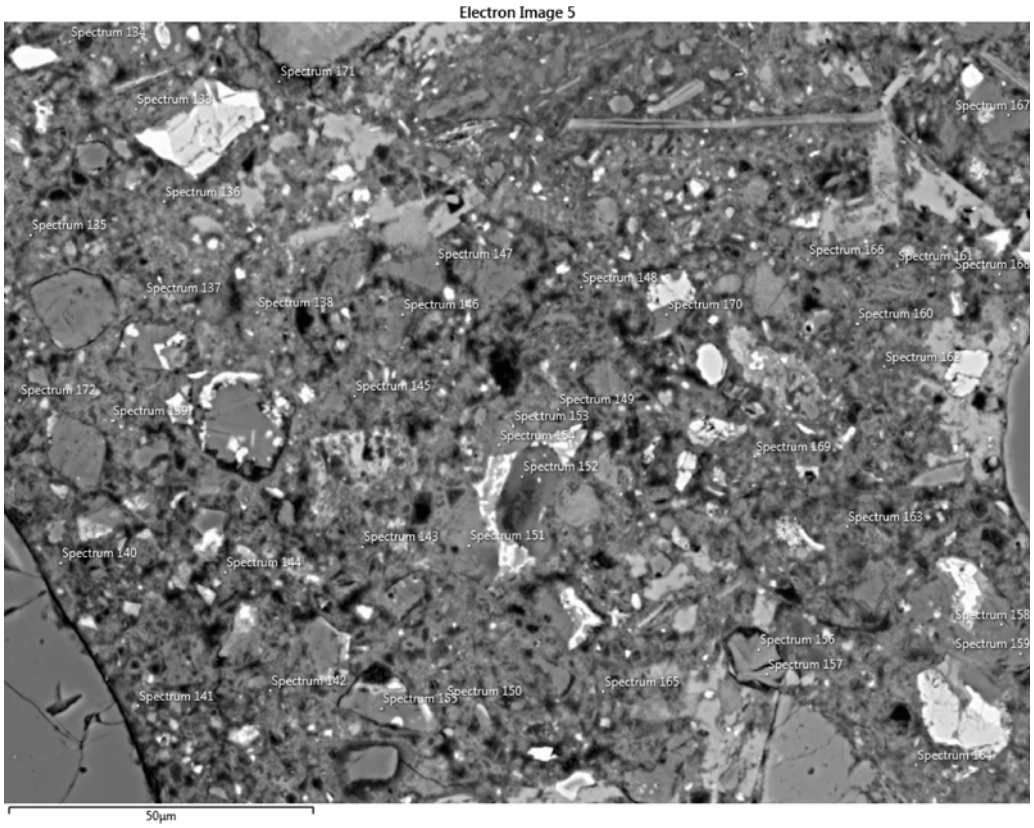

Fig. 7 - Microstructure of mortar sample 47; 65% β clinker + 30% fly ash D + 5% limestone

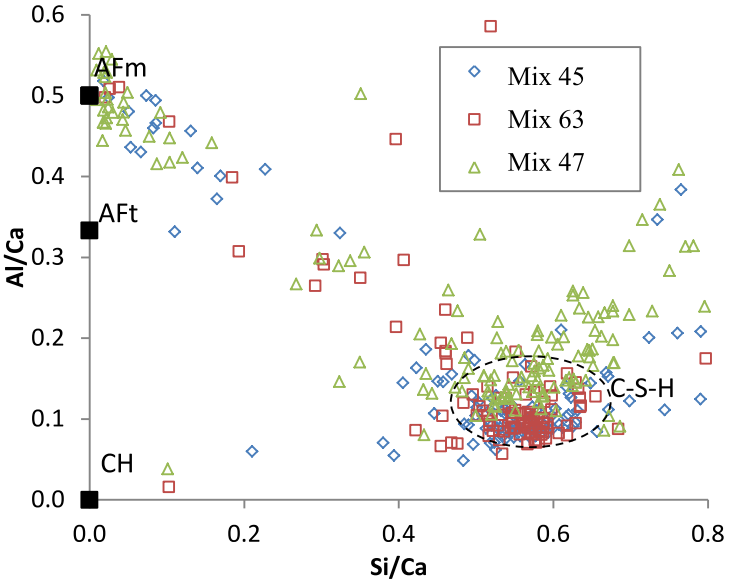

Fig. 8 - Al/Ca ration as function of Si/Ca ratio of the EDS point analyses of the different blended cements tested. This graph serves to identify the Ca/Si ration of the CSH and the aluminate uptake of the CSH as Al/Ca. In addition, AFm and AFt phases can be distinguished. Points from matrix of mortars 45, 63 and 47 are plotted here as diamond, square and triangles, respectively.

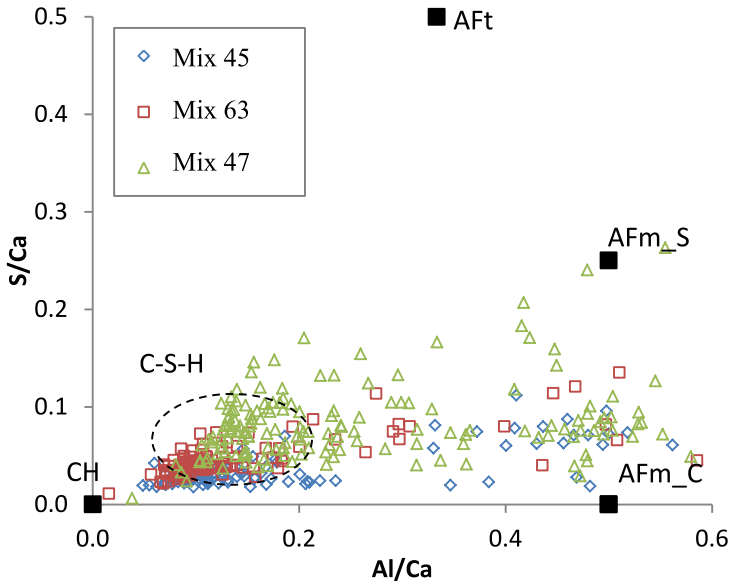

Fig. 9 - S/Ca ration as function of Al/Ca ratio of the EDS point analyses of the different blended cements tested. This graph serves to identify the sulphate containing AFm and AFt phases (AFt = ettringite, AFm_S = monosulphoaluminate and AFm_C = monocarboaluminate). Points from matrix of mortars 45, 63 and 47 are plotted here as diamond, square and triangles, respectively.

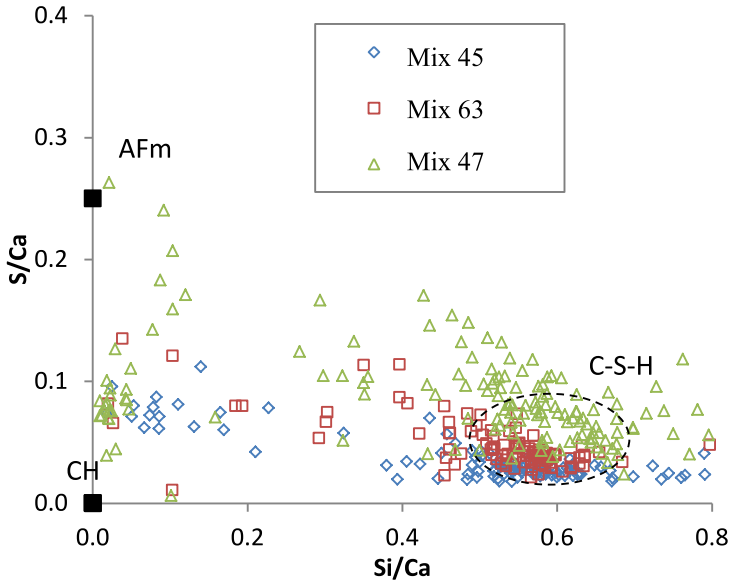

Fig. 10 - S/Ca ration as function of Si/Ca ratio of the EDS point analyses of the different blended cements tested. This graph serves to identify the Si/Ca ratio of the CSH and the sulphate uptake in the CSH. AFm represents monosulphate in this graph. Points from matrix of mortars 45, 63 and 47 are plotted here as diamond, square and triangles, respectively.